Protein-Based Multi-Mode Interference Optical Micro-Splitters

Yun-Lu Sun, Si-Ming Sun, Bo-Yuan Zheng, Zhi-Shan Hou, Pan Wang, Xu-Lin Zhang, Wen-Fei Dong, Lei Zhang, Qi-Dai Chen, Li-Min Tong, and Hong-Bo Sun, *Member, IEEE*

***Abstract*— Protein-based multi-mode interference optical micro-splitters (P-MMIs) were customized from bovine serum albumin aqueous ink by maskless and noncontact femtosecond laser direct writing. Good bio-/eco-compatibility could be achieved using protein-based biopolymers. As a premise of protein waveguide-based devices like P-MMIs, protein-based optical micro-waveguides were tested with ∼0.059-dB/μm transmission loss for more bio-transparent 633-nm light. With satisfactory implementation of micro/nano-scale structure details, prototyping P-MMIs (two device geometries designed for 532 nm and 633 nm respectively) were fabricated and operated well as fundamental integrated optical devices for light splitting for the first time to our knowledge.**

***Index Terms*— Biological materials, optics, micro/nano-waveguides, multi-mode interference optical micro-splitters.**

I. Introduction

RECENTLY, biopolymer-based optical waveguide devices are drawing increasing attention and effort for biosensing and biomedical applications motivated by their excellent biocompatibility, biodegradability, controllable mechanical flexibility, and facility of modification and functionalization [1]–[3]. In particular, biopolymer-based waveguide micro/nano-devices may bring about significant improvements in response speed [3], [4], integration [4], and portability [1], [3]. For the distinct advantages mentioned above as well as abundance, renewability, eco-friendliness, and diverse bio-functions, protein-based biopolymers (e.g., silk [2], [5], gelatin [3], albumins [6]–[8], . . .) are important and even irreplaceable in some situations among numerous artificially synthetic and natural-product polymeric materials, especially for promising novel hydrogel-based optics [2], [3], [5]–[8]. However, natrual proteins are not particularly "designed" for micro/nano-fabrication, especially photo-processing, which still needs improvements. So, especially via direct writing methods, protein-based optical waveguide devices were rarely reported to be endowed with sub-micro-scale or even nano-scale precision, or complicated device geometries [2]. This might be one "shortcoming" of protein-based biopolymers compared with well-exploited artificial synthetic polymers like resins. For instance, biopolymer-based micro/nano-scale optical splitters and couplers haven't been reported to be fabricated with high customizability and quality as far as we know, which could be widely applied in fields such as newfashioned optical micro/nano-biosensors [9], [10], multiplexed chemical and biological detection [11], and high-throughput integrated optofluidics [12], [13]. This may limit the improvement of integration level, high throughput and multiplexing, natural-product biomaterials' wide utilization, and multiple functionalization of biopolymer-based optics.

Therefore, In this Letter, we applied promising femtosecond laser direct writing (FsLDW) to fabricate the first batch of protein-based multi-mode interference optical micro-splitters (P-MMIs), a fundamental class of optical integrated devices [14], from bovine serum albumin (BSA) aqueous ink. By noncontact and maskless FsLDW, nanoscale processing resolution important for optical devices, relative facility of "one-step" fabrication, and good designability could be comprehensively and simply realized [15]–[17]. Besides, due to high space and time (fs-scale pulse width much shorter than thermal diffusion time) restriction of laser energy, controllable low collateral damage of FsLDW can be achieved even in complicated bio-environments [18]. And the bioactivity of functional protein molecules can be adjustably retained after FsLDW [18], [19], which might be greatly helpful for facile functionalization without complex subsequent modifications. Here, nanoscale spatial resolution (fine BSA nanowires with diameters as small as 150 nm) and good morphology (∼ 5-nm average roughness, Ra [7], [8]) were achieved by carefully optimized FsLDW. Then, prototyping P-MMIs were high-quality customized for different working wavelengths (633 nm and 532 nm for demonstration) with applicable light-splitting performance. Importantly for biorelated applications, both aqueous FsLDW-processing procedures and obtained P-MMIs show excellent biocompatibility via the approach applied here. These P-MMIs could be used as key elements for biopolymer-based integrated optical micro/nano-systems, multiplex high-throughput biodetection, as well as fields like eco-friendly biopolymer alternatives of artificial materials, and open new opportunities for integrated photonic/optical biosystems and bioengineering.

II. Fabrication

In the experiment, P-MMIs were directly "written" out on MgF_2 slices from BSA aqueous ink (BSA, 500 mg/mL;

Manuscript received September 13, 2015; revised October 16, 2015; accepted November 19, 2015. Date of publication November 24, 2015; date of current version February 18, 2016. This work was supported by the National Natural Science Foundation of China and National Basic Research Program of China under Grant 61137001, Grant 2011CB013005, Grant 91323301, Grant 91423102, and Grant 61435005.

The authors are with the State Key Laboratory on Integrated Optoelectronics, College of Electronic Science and Engineering, Jilin University, Changchun 130012, China (e-mail: chenqd@jlu.edu.cn; hbsun@jlu.edu.cn).

Color versions of one or more of the figures in this letter are available online at http://ieeexplore.ieee.org.

Digital Object Identifier 10.1109/LPT.2015.2503297

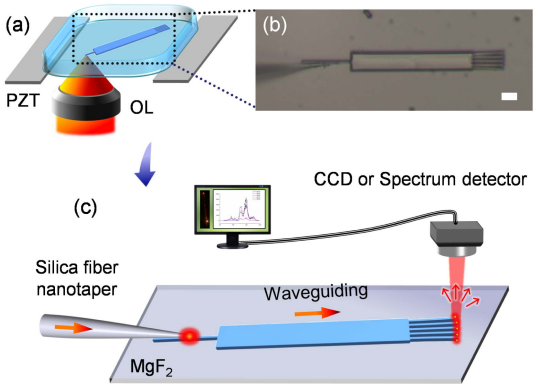

Fig. 1. (a) Schematic diagram of FsLDW of protein-based MMI micro-splitters. (b) Optical microscopic (OM) image of as-prepared protein-based MMI micro-splitters on MgF_2 substrate. Scale bar, 10 μm. (c) Schematic of the test of a protein-based MMI micro-splitter.

photosensitizer methylene blue, 0.6 mg/mL) by FsLDW as shown in schematic of Fig. 1 (a). Two-photon absorption of methylene blue (MB) occurred in the core region of laser beam focal spot (femtosecond laser, 80 MHz repetition rate, 120 fs pulse width, 790 nm central wavelength; oil-immersion objective lens (OL), 60×, numerical aperture, 1.35), and produced singlet oxygen ($^1O_2$). $^1O_2$ further induced crosslinking of BSA molecules with photopolymerizable groups (Tyr, Trp, His, Met, Cys, etc.) [6]–[8]. Combined with computer-programmed 3D scanning of the focused laser spot (vertical scanning by a piezo stage and horizontal scanning by a two-galvano-mirror set), arbitrarily designed waveguide micro/nano-devices could be FsLDW constructed on substrates after necessary water rinsing to remove residual BSA ink. In this work, MgF_2 substrate was applied for its lower refractive index (1.39) than that of FsLDW-fabricated protein hydrogels ($\sim$ 1.55 in air [6]–[8]), which met the requirements of total reflection and light propagation along the waveguide devices (see Fig. 1 (b)) [4]. With a silica fiber nano-taper, incident light was launched into the protein micro/nano-waveguides by evanescent field coupling as schematically illustrated in Fig. 1 (c). And the output light at the emitting ends of the waveguide devices could be captured and analyzed with a CCD camera or a spectrum detector.

During FsLDW processing, parameters such as laser power ($\sim$ 20 mW, measured before OL), exposure time (1000 μs at every point) and scanning step (100 nm in three dimensions (3D)) were sufficiently optimized to achieve good quality of morphology including as-designed device geometry and high surface smoothness ($\sim$5-nm Ra [7], [8]) [Fig. 2]. Importantly, the highly reproducible fine morphology was guaranteed by stable FsLDW system equipped with an output feedback system and proper enclosure. Additionally, the local temperature (22+/−0.2 °C) and humidity (relative humidity, $\sim$ 20%) around the laser was maintained constant in the super-clean lab. Therefore, protein-based micro/nano-waveguides and MMI micro-splitters could be customized by optimized FsLDW with high morphology quality, geometry faithfully as designed and satisfactory repeatability [Fig. 2]. In the scanning electron microscopy (SEM) image

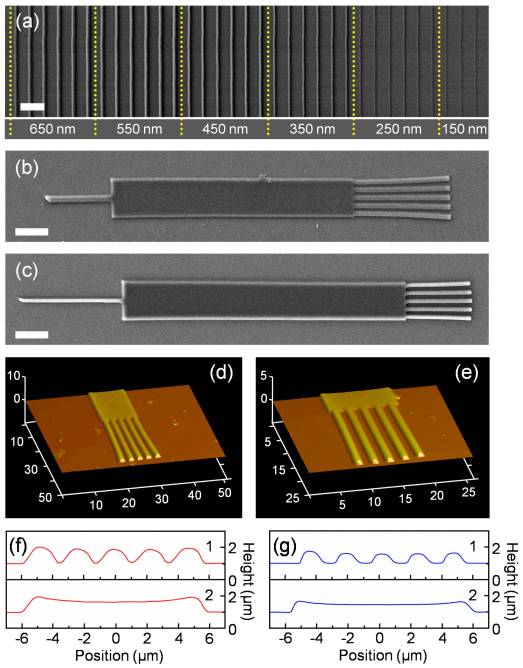

Fig. 2. (a) SEM image of one sample with sets of protein nanowires with diameters from $\sim$150 nm to $\sim$650 nm. Scale bar, 10 μm. SEM image of the protein-based MMI micro-splitter designed for (b) 633-nm and (c) 532-nm light. Scale bar, 10 μm. (d) AFM 3D detail of the protein-based MMI micro-splitter designed for 633-nm light (in air). Unit of coordinate: μm. (e) AFM 3D detail of the protein-based MMI micro-splitter designed for 532-nm light (in air). Unit of coordinate: μm. (f, g) Sectional profiles of (1) branch parts and (2) planar waveguides of protein-based micro-MMIs of (d) and (e), respectively.

of Fig. 2 (a), fine protein nanowires with diameters from 150 nm to 650 nm were written out as designed. The uniformity of every set of micro/nano-wires in Fig. 2 (a) well proved the good repeatability and controllability of positioning and geometry of protein-FsLDW. As a result of the nanoscale processing precision, P-MMIs with high quality were customized on MgF_2 substrate [Fig. 2 (b) and (c)]. With optimal processing parameters mentioned above, it took about 17 minutes to FsLDW fabricate a micro-MMI in Fig. 2 (b), and about 20 minutes for another micro-MMI in Fig. 2 (c). By atomic force microscopy (AFM) characterization [Fig. 2 (d) and (e)], surface Ra was measured to be $\sim$ 5 nm that is smooth enough for optical waveguiding applications [4]. Such high smoothness might be caused by so-called "self-smoothing" effect, which was helpful for achieving surface roughness much lower than voxel size [6]–[8]. In addition, P-MMIs exhibited good 3D geometries consistent with the design simultaneously considering optical performance, testing feasibility and quality control ($\sim$1-μm thickness) [Fig. 2 (d-g)].

III. Waveguiding Characteristics

In this work, much effort was put into FsLDW optimization to guarantee sufficient morphology and geometry quality for optical applications of protein-based biopolymer as the natural-product alternative of artificial polymers. It was because that the surface and 3D-shape were two key

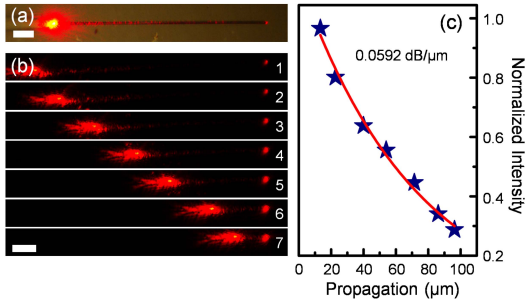

Fig. 3. (a) OM image of a protein micro-waveguide in air with 633-nm light launched and propagated in. Scale bar, 10 μm. (b) OM dark field images of different light propagation distances. Scale bar, 10 μm. (c) Points of normalized output intensities under different propagation distances (according to images of (b) 1-7) and exponentially fitted curve.

factors determining optical performances of waveguide-based elements. Based on the prerequisite of high-quality morphology described above, as-formed protein-based micro-waveguides could work satisfactorily. As shown in Fig. 3 (a), incident light from a 633-nm laser was evanescently coupled into a protein microwire with ~1-μm diameter and 100-μm length using a silica fiber nano-taper in air. Here, 633-nm light was emphatically used in tests because of its relatively high permeability and transparency for some biological tissues like adipose tissues, which might improve its potential for biomedical applications. The propagated light was output at the end of the protein micro-waveguide and was collected and measured. In Fig. 3 (b) 1-7, by changing the position where the incident light was launched in, it exhibited visually that the output light intensity was gradually diminished along with the increase of propagation distance. This normal phenomenon was caused by increased transmission loss corresponding to increased propagation distance. The gray values of images of output light were accumulated and normalized as the indexes of output intensities. Then the curve of normalized output intensities according to variational propagation distance were obtained in Fig. 3 (c). By exponentially fitting the data points in Fig. 3 (c), the transmission loss of the protein-based single microwire waveguide on MgF_2 was estimated to be ~ 0.059 dB/μm in air.

Here, residual MB (FsLDW photosensitizer) was absorbed and loaded on BSA molecules even after laser processing and water rinsing. For the BSA/MB hydrogel, light absorption and resulted transmission loss are higher at wavelength from ~ 550 nm to ~ 680 nm because of residual MB [20]. Actually, photosensitizers with lower light absorption could be applied for FsLDW (e.g., flavin adenine dinucleotide, FAD, owning high transparency for wavelengths longer than ~ 500 nm). On the other hand, the micro/nano-devices were constructed voxel by voxel during FsLDW. Although there is "self-smoothing" phenomenon via surface tension, it needs to take special efforts to ensure sufficiently high quality of as-obtained surfaces of protein-based micro/nano-devices [21]. Better FsLDW fabrication quality could be achieved via higher NA of objective lens, higher laser power, denser scanning, improved scanning mode, and higher protein concentration of FsLDW ink [21].

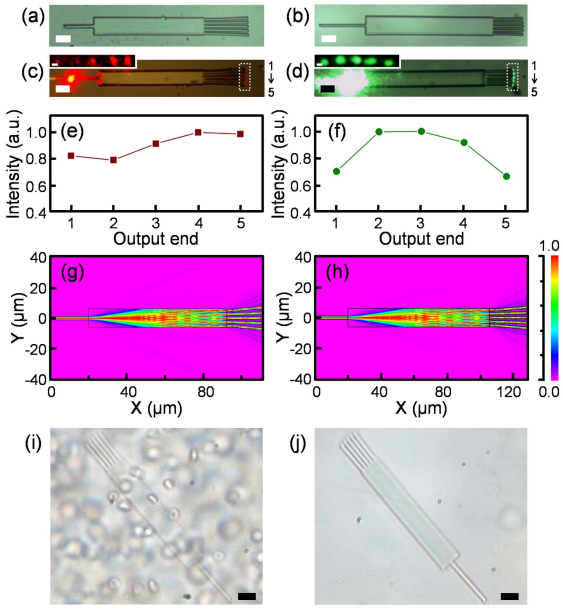

Fig. 4. OM image of a protein-based MMI designed for (a) 633-nm and (b) 532-nm light (scale bar, 10μm). Light-splitting tests of the protein-based MMI with (c) 633-nm and (d) 532-nm incident light (scale bar, 10 μm); insets, dark-field OM image of emitting ends 1~5 (scale bar, 1 μm). (e) Output light intensities from emitting ends 1~5 of the protein-based MMI in (c). (f) Output light intensities from emitting ends 1~5 of the protein-based MMI in (d). Rsoft simulation of a protein-based MMI designed for (g) 633-nm and (h) 532-nm light. (i, j) OM images of a BSA-based micro-MMI (i) during and (j) after 2-hour immersion in suspension solution of rat red blood cells (37 °C; scale bars, 10 μm).

Thus, some improvements for better light guiding performance may include in our future work: (i) long-wavelength working light source (e.g., near-infrared range over $\sim$ 700 nm), (ii) photosensitizers with lower absorption at operating wavelengths of guided light (e.g., FAD), and (iii) higher fabrication quality (mainly via further optimizing FsLDW).

IV. Light Splitting

Based on protein-based micro-waveguides achieved above, P-MMIs were designed and high-quality customized for 633-nm and 532-nm light respectively in Fig. 4 (a) and (b). For facile preliminary demonstration, 633-nm and 532-nm incident light was evanescently launched into P-MMIs respectively in Fig.4 (a) and (b) with nanoscale silica fiber tapers. Although this simple evanescent coupling method might be relatively rough and difficult to estimate insertion loss [4], these prototypes of P-MMI micro-devices show proper light splitting for their design wavelengths [see Fig. 4 (c) and (d)]. In Fig. 4 (e) and (f), the image gray values of emitting ends were accumulated and normalized respectively to exhibit the intensity distribution of divided light coupled and propagated in the multimode slab waveguide of P-MMIs (see insets and dashed regions of ends 1-5 in Fig. 4 (c) and (d)). For the P-MMI in Fig. 4 (c) for 633-nm light, the normalized output intensities of ends 1-5 ranged from $\sim$ 0.8 to 1.0 [Fig. 4 (e)]; for the P-MMI in Fig. 4 (d) for 532-nm light, the normalized output intensities of ends 1-5 ranged from $\sim$ 0.7 to 1.0 [Fig. 4 (f)]. Though the light-splitting performance needed

to be further improved, the first P-MMIs, as far as we know, were preliminarily realized as prototypes here.

As for the device designing, the approximate formula for the compact symmetric MMIs here is as follow [14],

$$L_{compact} \approx \frac{nW^2}{N\lambda}.$$

Here, $L_{compact}$ is the multimode waveguide length of compact type MMI, n is the refractive index (~ 1.55 for as-formed protein hydrogel in air [6]–[8] and approximate to the effective refractive index of 1-μm-thick protein-hydrogel film on MgF_2), W is the multimode waveguide width (12 μm here for multiple high-order modes), N is the number of output ends ($N = 5$ here), and λ is the design wavelength. Thus, approximately, for $\lambda = 633$ nm, $L_{compact} \approx 70.5$ μm; for $\lambda = 532$ nm, $L_{compact} \approx 83.9$ μm. Because of the approximation of the formula, Rsoft numerical simulation was adopted for optimized design so that $L_{compact} = 72.5$ μm for 633-nm light [Fig. 2 (e), Fig.4 (a) (c) and (g)] and $L_{compact} = 85.5$ μm for 532-nm light [Fig. 2 (f), Fig.4 (b) (d) and (h)] in air. The P-MMIs were fabricated by FsLDW precisely as designed, and therefore worked well in air and consistently with simulations [see Fig.4 (c) and (d)].

In addition, fine biocompatibility and anti-biofouling ability of these P-MMIs were preliminarily and experimentally proved by hemolysis tests. After immersion in aqueous dispersed suspension of rat red cells for 2 hours or longer (under rat body temperature of 37 °C in 0.9-wt%-NaCl normal saline), there was no impact on device morphology (no red cells adhered via good anti-biofouling of BSA hydrogels) or no obvious hemolysis [Fig.4 (i) and (j)] [7]. Similar anti-biofouling feature could be observed for P-MMIs immersed in mixture of broken red cells for hours (containing various proteins). Meanwhile, the protein-based micro/nano-elements can be directly "written" out in aqueous environments and right near to live cells or bacteria via the inimitably biocompatible and noncontact "in-situ" protein-FsLDW [18]. These features exhibit great promise of the FsLDW-fabricated P-MMIs for applications in complicated bio-related situations.

V. Conclusion

In summary, for the first time to our knowledge, we have reported the P-MMIs customized by FsLDW using BSA aqueous ink. The nanoscale quality control of device morphology and highly reproducible customization of the P-MMIs were guaranteed by carefully optimized and stabilized FsLDW. Transmission loss of a protein-based micro-waveguide was ~ 0.0592 dB/μm for 633-nm incident light launched in by evanescent field coupling, which is enough for optical biosensing for example of being FsLDW-integrated in traditional photonic micro/nano-systems as key functional components. Then, biocompatible prototyping P-MMIs were demonstrated experimentally to operate well as designed (two device geometries customized for 532 nm and 633 nm respectively) with applicable light-splitting performance. In short, the initial implementation of P-MMIs in this Letter shows application promise for environment-friendly biopolymer-based optics, multiplex and high-throughput optical biosensing, integrated and microminiaturized biophotonic systems like optofluidic biochips.

References

[1] M. Choi, J. W. Choi, S. Kim, S. Nizamoglu, S. K. Hahn, and S. H. Yun, "Light-guiding hydrogels for cell-based sensing and optogenetic synthesis *in vivo*," *Nature Photon.*, vol. 7, no. 12, pp. 984–987, 2013.

[2] S. T. Parker *et al.*, "Biocompatible silk printed optical waveguides," *Adv. Mater.*, vol. 21, no. 23, pp. 2411–2415, 2009.

[3] A. K. Manocchi, P. Domachuk, F. G. Omenetto, and H. Yi, "Facile fabrication of gelatin-based biopolymeric optical waveguides," *Biotechnol. Bioeng.*, vol. 103, no. 4, pp. 725–732, 2009.

[4] P. Wang, Y. Wang, and L. Tong, "Functionalized polymer nanofibers: A versatile platform for manipulating light at the nanoscale," *Light, Sci. Appl.*, vol. 2, no. 10, p. e102, 2013.

[5] F. G. Omenetto and D. L. Kaplan, "New opportunities for an ancient material," *Science*, vol. 329, pp. 528–531, Jul. 2010.

[6] Y.-L. Sun *et al.*, "Protein-based soft micro-optics fabricated by femtosecond laser direct writing," *Light, Sci. Appl.*, vol. 3, no. 1, p. e129, 2014.

[7] Y.-L. Sun *et al.*, "Dynamically tunable protein microlenses," *Angew. Chem.*, vol. 124, no. 7, pp. 1590–1594, 2012.

[8] Y.-L. Sun, D.-X. Liu, W.-F. Dong, Q.-D. Chen, and H.-B. Sun, "Tunable protein harmonic diffractive micro-optical elements," *Opt. Lett.*, vol. 37, no. 14, pp. 2973–2975, 2012.

[9] A. Ymeti *et al.*, "Fast, ultrasensitive virus detection using a Young interferometer sensor," *Nano Lett.*, vol. 7, no. 2, pp. 394–397, 2007.

[10] K. R. Kribich *et al.*, "Novel chemical sensor/biosensor platform based on optical multimode interference (MMI) couplers," *Sens. Actuators B, Chem.*, vol. 107, no. 1, pp. 188–192, 2005.

[11] S. Chakravarty *et al.*, "Multiplexed specific label-free detection of NCI-H358 lung cancer cell line lysates with silicon based photonic crystal microcavity biosensors," *Biosensors Bioelectron.*, vol. 43, pp. 50–55, May 2013.

[12] Y. Zou, S. Chakravarty, W. C. Lai, C. Y. Lin, and R. T. Chen, "Methods to array photonic crystal microcavities for high throughput high sensitivity biosensing on a silicon-chip based platform," *Lab Chip*, vol. 12, no. 13, pp. 2309–2312, 2012.

[13] C. F. Carlborg *et al.*, "A packaged optical slot-waveguide ring resonator sensor array for multiplex label-free assays in labs-on-chips," *Lab Chip*, vol. 10, no. 3, pp. 281–290, 2010.

[14] L. B. Soldano and E. C. M. Pennings, "Optical multi-mode interference devices based on self-imaging: Principles and applications," *J. Lightw. Technol.*, vol. 13, no. 4, pp. 615–627, Apr. 1995.

[15] H. Xia *et al.*, "Ferrofluids for fabrication of remotely controllable micro-nanomachines by two-photon polymerization," *Adv. Mater.*, vol. 22, no. 29, pp. 3204–3207, 2010.

[16] K. K. Seet, V. Mizeikis, S. Matsuo, S. Juodkazis, and H. Misawa, "Three-dimensional spiral-architecture photonic crystals obtained by direct laser writing," *Adv. Mater.*, vol. 17, no. 5, pp. 541–545, 2005.

[17] W. Xiong *et al.*, "Simultaneous additive and subtractive three-dimensional nanofabrication using integrated two-photon polymerization and multiphoton ablation," *Light, Sci. Appl.*, vol. 1, no. 4, p. e6, 2012.

[18] B. Kaehr and J. B. Shear, "Multiphoton fabrication of chemically responsive protein hydrogels for microactuation," *Proc. Nat. Acad. Sci. United States Amer.*, vol. 105, no. 26, pp. 8850–8854, 2008.

[19] S. Basu and P. J. Campagnola, "Enzymatic activity of alkaline phosphatase inside protein and polymer structures fabricated via multiphoton excitation," *Biomacromolecules*, vol. 5, no. 2, pp. 572–579, 2004.

[20] Y.-L. Sun *et al.*, "Customization of protein single nanowires for optical biosensing," *Small*, vol. 11, no. 24, pp. 2869–2876, 2015.

[21] Y.-L. Sun *et al.*, "Protein-based three-dimensional whispering-gallery-mode micro-lasers with stimulus-responsiveness," *Sci. Rep.*, vol. 5, p. 12852, Aug. 2015.